On the Seasonality of Arctic Black Carbon

ZHAOYI SHEN

Program in Atmospheric and Oceanic Sciences, Princeton University, Princeton, New Jersey

YI MING, LARRY W. HOROWITZ, AND V. RAMASWAMY

NOAA/Geophysical Fluid Dynamics Laboratory, Princeton, New Jersey

MEIYUN LIN

Program in Atmospheric and Oceanic Sciences, Princeton University, Princeton, New Jersey

(Manuscript received 5 August 2016, in final form 2 March 2017)

ABSTRACT

Arctic haze has a distinct seasonal cycle with peak concentrations in winter but pristine conditions in summer. It is demonstrated that the Geophysical Fluid Dynamics Laboratory (GFDL) atmospheric general circulation model (AM3) can reproduce the observed seasonality of Arctic black carbon (BC), an important component of Arctic haze. The model is used to study how large-scale circulation and removal drive the seasonal cycle of Arctic BC. It is found that despite large seasonal shifts in the general circulation pattern, the transport of BC into the Arctic varies little throughout the year. The seasonal cycle of Arctic BC is attributed mostly to variations in the controlling factors of wet removal, namely the hydrophilic fraction of BC and wet deposition efficiency of hydrophilic BC. Specifically, a confluence of low hydrophilic fraction and weak wet deposition, owing to slower aging process and less efficient mixed-phase cloud scavenging, respectively, is responsible for the wintertime peak of BC. The transition to low BC in summer is the consequence of a gradual increase in the wet deposition efficiency, whereas the increase of BC in late fall can be explained by a sharp decrease in the hydrophilic fraction. The results presented here suggest that future changes in the aging and wet deposition processes can potentially alter the concentrations of Arctic aerosols and their climate effects.

1. Introduction

The discovery of accumulation of visibility-reducing aerosols in the Arctic during late winter and early spring (known as Arctic haze) dates back to the late 1800s (Garrett and Verzella 2008, and references therein). After being underappreciated for decades, the haze was rediscovered by pilots flying over the North American Arctic in the 1950s (Mitchell 1957). Since then the haze has been attracting interests among researchers. The haze has its root cause in the long-range transport of air pollution originating from the midlatitude industrial regions (Barrie 1986) and can have an influence on Arctic climate (Law and Stohl 2007). The haze is a mixture of both light-scattering and light-absorbing aerosols. Black carbon (BC), which accounts for most of the aerosol absorption (Law and Stohl 2007), is a minor but important component of Arctic haze. BC poses strong positive radiative perturbations by absorbing solar radiation, by interacting with clouds, and by reducing the surface albedo when deposited onto snow and ice (Quinn et al. 2007). The surface temperature in the Arctic increased more than the global average since the late twentieth century, coinciding with a rapid decline of sea ice (Bindoff et al. 2013). Besides greenhouse gases, increased BC and decreased scattering aerosols (e.g., sulfate) in the Arctic due to the long-term emission trends were postulated to have contributed to this amplified Arctic climate change (Shindell and Faluvegi 2009).

A distinct seasonal cycle of Arctic BC concentrations is present in measurements. Long-term surface observations at Alert and Barrow show that BC concentrations tend to peak during late winter and early spring before starting to decline in April, and reach a minimum during summer (Sharma et al. 2006). Recent aircraft measurements of BC have shown that the seasonal change in BC vertical structures is in agreement with the seasonality of

Corresponding author: Zhaoyi Shen, zs@princeton.edu

DOI: 10.1175/JCLI-D-16-0580.1

surface concentrations (Koch et al. 2009; Eckhardt et al. 2015). Different seasonally dependent mechanisms, such as atmospheric transport and removal, have been posited to explain the seasonal cycle of Arctic BC.

Previous studies have shown that similar to other aerosols, Arctic BC is dominated by emissions from Europe and the Asian part of Russia, with smaller contributions from East Asia and North America (e.g., Stohl 2006; Shindell et al. 2008). A dynamically oriented view holds that during the haze season (winter and spring), meridional transport from midlatitude source regions to the Arctic is stronger because of vigorous large-scale circulation. The presence of Siberian high pressure helps steer polluted European air into the Arctic by transient and stationary eddies (Barrie 1986; Iversen and Joranger 1985). Using a Lagrangian particle dispersion model, Stohl (2006) has shown that in winter the diabatic cooling of air traveling over ice and snow facilitates penetration of the polar dome (surface of constant potential temperature) and transport to the Arctic lower troposphere. In contrast, pollution is diabatically transported to higher altitudes and diluted in summer (Klonecki et al. 2003). On the other hand, Ma et al. (2013) has shown that the circulation features do not have a strong effect on surface concentrations of Arctic BC in the Community Atmosphere Model.

Another mechanism that contributes to the seasonality of Arctic BC is the slower removal in winter. As a major sink term for aerosols, wet scavenging by precipitation (rain and snow) is modulated heavily by cloud microphysics. BC particles become effective ice nuclei (IN) only when the temperature is below approximately 240 K (Friedman et al. 2011) and is thus not effectively removed by ice clouds. In mixed-phase clouds, the Bergeron process (i.e., evaporation of liquid droplets in the presence of ice crystals) releases aerosols contained in cloud droplets back into air (Cozic et al. 2008), so the wet scavenging in mixed-phase clouds is much less efficient than in liquid clouds. The low efficiency of ice cloud and mixed-phase cloud scavenging favors accumulation of aerosols at cold temperatures. Previous studies have found that different treatments of aerosol removal in models are a leading cause of the spread in simulated BC burdens. Improving the wet deposition scheme in models has been shown to significantly increase Arctic BC burdens in winter and thus result in better simulation of the seasonal cycle (e.g., Liu et al. 2011; Bourgeois and Bey 2011; Browse et al. 2012; Wang et al. 2013). Dry deposition also has seasonal variations and is weaker in winter when the stable boundary layer inhibits turbulent mixing (Quinn et al. 2007). It, however, accounts for only a small portion of the total removal and affects mainly the surface concentrations of Arctic haze (Liu et al. 2011). Another key factor determining BC concentrations is the aging process, which refers to the transformation from hydrophobic to hydrophilic aerosols resulting from coating by soluble species (Petters et al. 2006). Only aged BC particles can act as cloud condensation nuclei (CCN) and be removed by in-cloud scavenging. As a result, the aging rate has a large effect on global BC concentrations and distributions. Previous studies have shown that incorporating microphysical process into treatment of the aging process yields a slower aging rate in winter and improves the models' capability in simulating the seasonal cycle of Arctic BC (Liu et al. 2011, 2016).

It is important to note that the aforementioned mechanisms (viz., large-scale circulation, cloud microphysics, and aging) are not mutually exclusive; they could all act to induce seasonality. Yet, the relative importance of these mechanisms in shaping the pronounced seasonal cycle of Arctic BC remains unclear. Although we have a general understanding of how air pollution is transported from the midlatitudes to the Arctic, transport of BC into the Arctic has not been quantified in the literature. On the other hand, most of the current modeling studies confirm the importance of wet deposition by investigating the sensitivity of simulated BC concentrations to different removal schemes. This approach, however, does not rule out the potential influence of transport on the seasonality of Arctic BC. In this paper we seek to provide a comprehensive analysis of the roles of long-range transport and wet removal in controlling the seasonal cycle of Arctic BC by quantifying BC budgets in the Arctic.

2. Model description

This study uses a modified version of the Geophysical Fluid Dynamics Laboratory (GFDL) atmospheric general circulation model (AGCM) AM3 (Donner et al. 2011) with a cubed-sphere grid resolution of about 100 km and 48 hybrid vertical levels from the surface to approximately 1 Pa. We conduct a 6-yr hindcast simulation (2008–13), following one year of spinup. The emission inventories reflect 2008–13 conditions. Anthropogenic emissions of aerosol and ozone precursors with seasonal variations are based on Hemispheric Transport of Air Pollution (HTAP) theme 2—a mosaic of regional and global emission inventories for the years from 2008 to 2010 (Janssens-Maenhout et al. 2015)—and are held constant after 2010. Daily resolving biomass burning emissions for 2008–13 are adopted from the Fire Inventory from National Center for Atmospheric Research (NCAR) (FINN; Wiedinmyer et al. 2011) and emitted in the surface layer. The model is forced with observed sea surface temperatures and sea ice, and horizontal winds are nudged to the National Centers for Environmental

Prediction (NCEP) Global Forecast System Reanalysis at approximately 1.4° × 1.4° horizontal resolution using a pressure-dependent nudging technique (Lin et al. 2012). The latter makes it possible to compare model simulations with observations for specific flight campaigns.

AM3 uses a bulk aerosol scheme and calculates the mass of aerosols based on their emissions, chemical reactions, transport, and wet and dry deposition, as described by Donner et al. (2011). Here we describe briefly the treatment of wet deposition, which is most pertinent to this study. In AM3, all aerosols are treated as externally mixed, and prescribed lognormal size distributions are assumed for computing aerosol activation into cloud droplets. Wet deposition includes in- and below-cloud scavenging by large-scale and convective clouds. For in-cloud scavenging of hydrophilic aerosols, the removal rate is equal to the scavenging efficiency (i.e., the fraction of aerosols that is incorporated into cloud droplets or ice crystals and removed by precipitation) multiplied by the fractional conversion rate of cloud condensate to precipitation. The scavenging efficiency is prescribed for each aerosol type, with consideration of its solubility. In AM3, in-cloud scavenging does not depend on size explicitly. Below-cloud scavenging is considered only for large-scale precipitation and is parameterized following Li et al. (2008).

The treatment of BC in the modified AM3 used in this study has been discussed extensively by Liu et al. (2011) and Fan et al. (2012); here we summarize briefly the key features. The model includes two types of BC: hydrophobic (BCpo) and hydrophilic (BCpi). 80% (40%) of BC emitted from anthropogenic (biomass burning) sources is assumed to be hydrophobic. The hydrophobic BC is then converted to the hydrophilic form at a variable aging rate (Liu et al. 2011). BC aging is assumed to result primarily from the condensation of H_2SO_4 onto BC aerosol surface, a common process that has been examined extensively in observational and laboratory studies. H_2SO_4 is produced from the gas-phase oxidation of SO_2 by the OH radical and is rapidly converted to aerosol phase via nucleation or condensation onto existing particles. If it is assumed that during the transport of a plume the mixing with ambient air dilutes the concentrations of SO_2 and aerosols at the same rate, one can treat their ratio as a constant. As such, the aging rate is parameterized to be proportional to OH concentrations only, with the implicit assumption that there are always SO_2 and aerosol surface available for H_2SO_4 production. Aging can also occur through other processes (e.g., coagulation), which are believed to be slower and less important than condensation during long-range transport (Oshima et al. 2009). Their collective effect is represented by adding a small constant term to the parameterized aging rate coefficient. The final form of the aging process is

$$k_a = \beta[\mathrm{OH}] + \delta, \tag{1}$$

where k_a is the aging rate coefficient, and β and δ control the fast and slow aging processes, respectively. In AM3 β (which takes into account the effects of SO_2 and aerosol surface) is set to yield an *e*-folding aging time of 2.5 days under global mean OH concentrations, and δ is set by assuming a fixed *e*-folding time of 20 days for the slow aging processes.

Only hydrophilic BC can be removed by in-cloud scavenging, which is parameterized using a first-order rate coefficient k_{scav} (s^{-1}) (Fan et al. 2012):

$$k_{\mathrm{scav}} = \frac{F_{\mathrm{scav},1}P_{\mathrm{rain}} + F_{\mathrm{scav},2}(1-f_{\mathrm{berg}})P_{\mathrm{snow}} + F_{\mathrm{scav},3}f_{\mathrm{berg}}P_{\mathrm{snow}}}{Q_{\mathrm{liq}} + Q_{\mathrm{ice}}}, \tag{2}$$

where P_{rain} and P_{snow} are the three-dimensional rain and snow rates ($\mathrm{kg\,m^{-3}\,s^{-1}}$), respectively, and Q_{liq} and Q_{ice} are the liquid and ice cloud water content ($\mathrm{kg\,m^{-3}}$), respectively. Also, $F_{\mathrm{scav},i}$ is the scavenging efficiency for precipitation type i ($i = 1, 2, 3$), and f_{berg} is the fraction of snow produced by the Bergeron process. In this study, $F_{\mathrm{scav},1}$ and $F_{\mathrm{scav},2}$ are set to 0.2, and $F_{\mathrm{scav},3}$ is set to 0.01 to account for the less efficient removal of aerosols by snow produced by the Bergeron process than by rain and snow produced by riming and homogeneous freezing. Both hydrophobic and hydrophilic BC can be removed by below-cloud scavenging and dry deposition. The dry deposition velocity is calculated using the empirical resistance-in-series method with a surface-dependent collection efficiency (Gallagher 2002), resulting in a much smaller dry deposition velocity over snow and ice than over land surfaces (soils and canopy).

TABLE 1. Global and Arctic annual mean BC budgets in AM3.

	Emission ($\mathrm{Tg\,yr^{-1}}$)	Wet deposition ($\mathrm{Tg\,yr^{-1}}$)	Dry deposition ($\mathrm{Tg\,yr^{-1}}$)	Burden ($\mathrm{mg\,m^{-2}}$)
Global	7.5	4.0	3.5	0.31
Arctic	0.0052	0.078	0.012	0.12

Table 1 shows AM3-simulated global and Arctic BC budgets. The global BC emission (7.5 $\mathrm{Tg\,yr^{-1}}$) is close to the commonly used values of the industrial-era emission in the Aerosol Comparisons between Observations and Models (AEROCOM) project (Schulz et al. 2006) and is within the range of 4.7–11.4 $\mathrm{Tg\,yr^{-1}}$ in previous studies. The ratio of wet deposition to dry deposition of BC is 1.14, which lies toward the lower end of the published range (e.g., Koch 2001; Koch and Hansen 2005; Wang

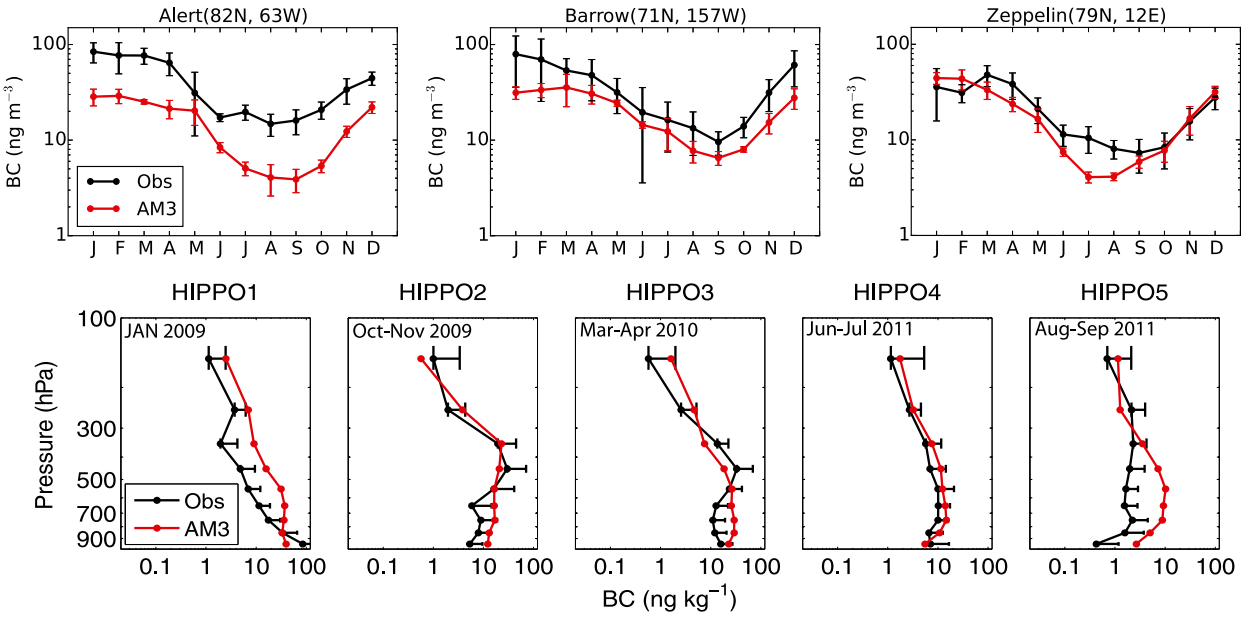

FIG. 1. (top) Model-simulated and observed monthly mean surface BC at (left)–(right) Alert (2008–12), Barrow (2008–13), and Zeppelin (2008–13). Error bars denote one std dev from monthly means. (bottom) Model-simulated and observed BC vertical profiles at high latitudes (66°–85°N) during HIPPO [HIPPO1 (January 2009), HIPPO2 (October–November 2009), HIPPO3 (March–April 2010), HIPPO4 (June–July 2011), and HIPPO5 (August–September 2011)]. Error bars associated with observational profiles represent one std dev of the HIPPO data. For the comparison, daily BC fields archived from the model are first sampled along the flight track and then averaged over 66°–85°N for each campaign.

et al. 2014). This may be related to the weak convective removal of aerosols in AM3 (Paulot et al. 2016), an issue that does not have a direct effect on wet deposition in the Arctic where large-scale precipitation dominates. It may result, however, in stronger high-altitude transport of aerosols in AM3 than in other models. The global mean column burden of BC (0.31 mg m^{-2}) is roughly in the middle of the range of previous model estimates (0.11–0.53 mg m^{-2}; Bond et al. 2013). Relatively few studies have provided BC budget terms in the Arctic. Local BC emissions are very small as expected. The Arctic mean BC column burden in AM3 (0.12 mg m^{-2}) is very similar to that estimated with the Community Atmosphere Model in a recent study (0.13 mg m^{-2}; Jiao and Flanner 2016). Wet deposition accounts for more than 85% of the total sink of BC in the Arctic, consistent with previous studies which have shown that wet deposition is the dominant removal pathway of aerosols in remote regions (e.g., Huang et al. 2010; Wang et al. 2014).

3. Simulated and observed seasonal cycle of Arctic BC

While the model treatment of aerosol transport and deposition processes has been improved considerably in recent years and most current models can qualitatively reproduce the seasonal variations of Arctic BC, large biases remain in the amplitudes of simulated seasonal cycles (Shindell et al. 2008; Eckhardt et al. 2015). Figure 1 shows AM3-simulated and observed monthly mean BC surface concentrations at Alert, Barrow, and Zeppelin (Eleftheriadis et al. 2009; Sharma et al. 2004, 2006). Measured BC exhibits similar seasonal variations at all three stations. Its concentrations peak in winter or early spring, followed by a rather precipitous decrease in April and May. The lowest concentrations occur from June to October. On average, BC concentrations in winter (DJF) are higher than in summer (JJA) by a factor of 3–4. The model is able to capture the seasonal cycle, but appears to underestimate BC at Alert and Barrow by a factor of 2–3 throughout the year. The performance of AM3 in simulating surface BC in the Arctic is comparable to the models in the Arctic Monitoring and Assessment Programme (AMAP), which underestimate BC at Alert and Barrow by about a factor of 2 on average, with largest biases during the haze season (Eckhardt et al. 2015). The discrepancy between AM3 and observations may result from model deficiencies, including uncertainties in BC emissions and deposition, or from observational errors, as some of the measurements are indirect and may be subject to rather large biases (Bond et al. 2013).

Figure 1 also compares the simulated BC vertical profiles at high latitudes (66°–85°N) with the aircraft measurements made during the High-Performance

Instrumented Airborne Platform for Environmental Research (HIAPER) Pole-to-Pole Observations (HIPPO) campaigns (Schwarz et al. 2013; Wofsy et al. 2011). The seasonal variations are evident in the data. In January, high concentrations of BC are confined within the boundary layer (HIPPO1). During early spring, there are enhancements of BC at higher altitudes (HIPPO3). BC concentrations at all altitudes start to decrease in June, and remain low throughout summer (HIPPO4 and HIPPO5). Despite some mismatches, AM3 generally reproduces the seasonal variations in BC vertical profiles. Previous studies have found no systematic bias in model-simulated free-troposphere BC when compared with aircraft observations (e.g., Koch et al. 2009; Eckhardt et al. 2015). Yet comparisons of BC vertical profiles are limited by a lack of spatial and temporal coverage of aircraft campaigns, and additional observations are needed for further model validation.

Based on the above results, we conclude that despite the remaining discrepancies between the model and observations, the performance of AM3 in simulating Arctic BC is similar to that of the current generation of models. AM3 is capable of reproducing the seasonal cycle of Arctic BC and thus can be used to study its underlying mechanisms. The improvement in AM3-simulated Arctic BC [compared to the standard version in Donner et al. (2011)] is attributed to the modified BC-related processes (aging, wet removal, and dry deposition) in the model, and Liu et al. (2011) discussed the sensitivity of BC simulation to each process in detail. Since observations show similar seasonality of Arctic BC at the surface and in the free troposphere, we will focus on the BC column burden averaged over the Arctic for the rest of the paper. This allows us to take full advantage of the model and generalize the results to the entire Arctic. The column burden is also more relevant to the radiative effects of BC than the surface concentrations, and has received much attention in the literature.

4. Controlling factors of Arctic BC

We employ a box model of the Arctic region to quantify the key factors controlling Arctic BC concentrations. Given the relatively small emissions from local sources, the prevailing balance is between the meridional BC transport into the Arctic and local deposition. One can write the rate of change in the average BC column burden C ($\mathrm{kg\,m^{-2}}$) as

$$\frac{dC}{dt} = \frac{F}{S} - W - D, \tag{3}$$

where F is the total net meridional flux into the Arctic ($\mathrm{kg\,s^{-1}}$), S is the Arctic surface area ($\mathrm{m^2}$), and W and D are the average wet and dry deposition rates ($\mathrm{kg\,m^{-2}\,s^{-1}}$), respectively. Note that F includes transport into and out of the Arctic. Since the dry deposition of BC and the below-cloud scavenging of BCpo in the Arctic region are small (around 10% of the total BC deposition in the Arctic in the model simulation; see Table 1) and can be neglected, Eq. (3) can be simplified as

$$\frac{dC}{dt} = \frac{F}{S} - W_{\mathrm{pi}}, \tag{4}$$

where W_{pi} is the average BCpi wet deposition rate ($\mathrm{kg\,m^{-2}\,s^{-1}}$). Note that W_{pi} can be written as rwC, where r represents the dimensionless hydrophilic fraction of BC C_{pi}/C, (with C_{pi} being the average BCpi column burden) and w represents the wet deposition efficiency of BCpi $W_{\mathrm{pi}}/C_{\mathrm{pi}}$ ($\mathrm{s^{-1}}$), which can be thought of as the BCpi concentration-weighted in-cloud scavenging rate coefficient k_{scav} defined in Eq. (2), and is different from the wet scavenging efficiency $F_{\mathrm{scav},i}$. Here r and w are derived from column-integrated quantities, and require no assumption regarding the vertical distributions of BCpi and BCpo. As the AM3-simulated residence time of Arctic BC ranges from 6 to 20 days depending on the season (not shown), we assume a steady state on the monthly time scale and arrive at an expression for C:

$$C = \frac{F}{Srw}. \tag{5}$$

An inspection of Eq. (5) suggests that elevated BC concentrations could result from stronger transport from midlatitude source regions and/or weaker wet removal. General circulation patterns are important for determining long-range transport fluxes. Wet removal is reduced when a smaller fraction of BC is hydrophilic or the wet deposition efficiency of BCpi is lower. The aging process exerts a strong control over the hydrophilic fraction. The wet deposition efficiency is affected mainly by the phase of precipitation because in-cloud scavenging efficiency differs among liquid, ice, and mixed-phase clouds.

We apply the box model to quantify the roles of the three main variables, namely the meridional BC flux F, BC hydrophilic fraction r, and BCpi wet deposition efficiency w, in controlling the seasonality of Arctic BC. The monthly mean values of F, r, and w averaged over the Arctic (defined as poleward of 66°N) are computed from our AM3 simulation. Figure 2a compares the monthly mean BC column burdens calculated using the box model with AM3 simulations. The good agreement validates the assumptions made in deriving Eq. (5). The box model captures the seasonal cycle, suggesting that

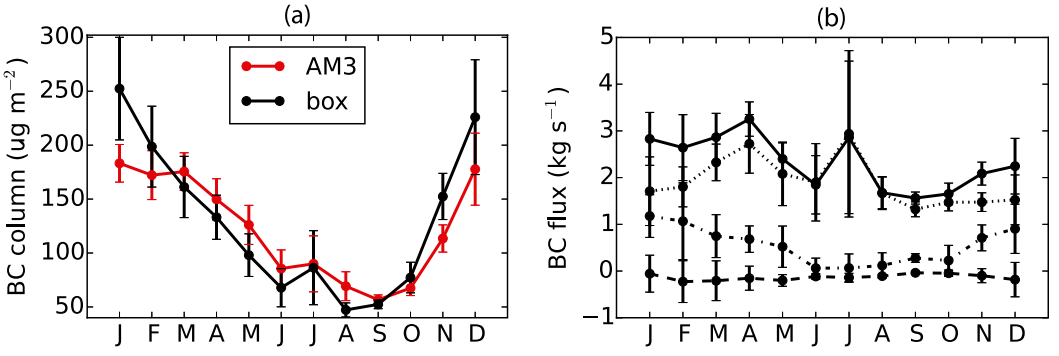

FIG. 2. Monthly mean (a) Arctic BC column burdens simulated using AM3 (red) and derived from the box model (black), and (b) AM3-simulated total meridional BC flux into the Arctic (solid) and contributions from the mean meridional circulation (dashed), stationary eddies (dashed–dotted), and transient eddies (dotted). Error bars denote one std dev from monthly means.

one can rationalize the seasonality of Arctic BC by examining the three variables defined above.

5. Meridional transport

Like other anthropogenic aerosol species, BC is emitted mainly at the midlatitude industrial regions and carried into the Arctic by atmospheric transport. Isentropic airflow facilitates high-level transport from warm and humid (high equivalent potential temperature θ_e) areas such as North America and East Asia, and low-level transport from comparatively low θ_e areas such as Europe (Stohl 2006). Cross-isentropic transport due to diabatic heating or cooling also plays an important role (Klonecki et al. 2003). The total meridional BC flux F can be decomposed into contributions from the mean meridional circulation (MMC), stationary eddies, and transient eddies:

$$\{\overline{vc}\} = \underbrace{\{[\overline{v}][\overline{c}]\}}_{\text{MMC}} + \underbrace{\{\overline{v}^*\overline{c}^*\}}_{\text{stationary eddies}} + \underbrace{\{\overline{v'c'}\}}_{\text{transient eddies}}, \quad (6)$$

where v is the meridional wind velocity (m s^{-1}), and c is the BC mass mixing ratio (kg kg^{-1}). Overbars denote monthly means, square brackets zonal means, primes deviations from monthly means, asterisks deviations from zonal means, and curly brackets zonal and vertical integrals (from the surface to ~100 hPa). Figure 2b shows the annual cycle of the total monthly mean meridional BC flux into the Arctic (at 66°N) and its three components. Generally, the total BC flux does not show much variation with time. The average flux is only about 20% higher in DJF than in JJA, far from sufficient to account for the column burden difference between the two seasons (Fig. 2a). The contribution of the mean meridional circulation is very small. The transport is realized almost entirely by the eddy components. The flux by stationary eddies is comparable to that by transient eddies in DJF, while the latter dominates in JJA.

Although the vertically integrated BC flux changes little throughout the year, its vertical structure does vary with the season (Fig. 3). The flux in DJF is characterized by two peaks (one in the boundary layer, and the other at about 500 hPa), which are of different origins. In winter the polar dome extends to about 40°N, allowing the low-level transport of BC from Europe (Stohl 2006). The diabatic cooling occurring when relatively warm air travels over a cold surface (i.e., strong inversion) keeps European BC in the boundary layer. The flux at about 500 hPa is more likely to be a result of transport from lower-latitude regions such as East Asia and North America. In

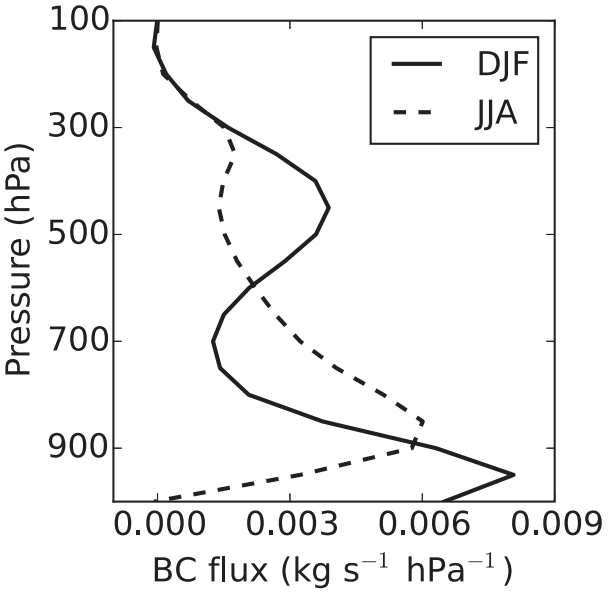

FIG. 3. Vertical profiles of meridional BC flux at 66°N. The solid and dashed lines represent DJF and JJA, respectively.

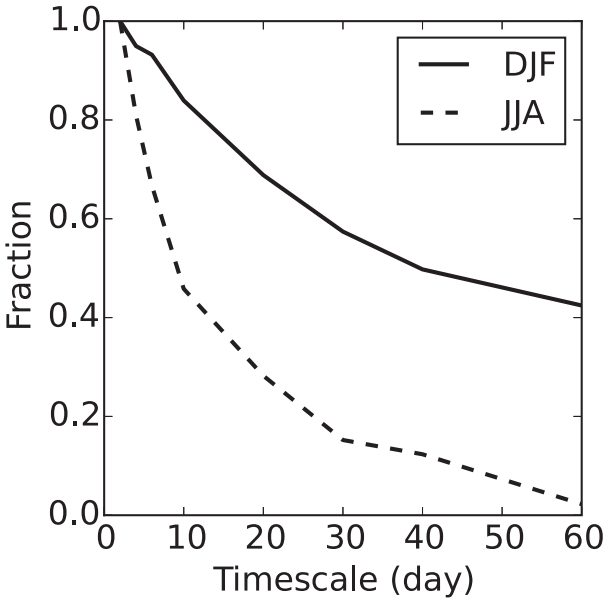

FIG. 4. Time-filtered meridional BC flux $\{\overline{v_n c_n}\}$ (defined in section 5) as a fraction of total flux at 66°N. The solid and dashed lines represent DJF and JJA, respectively.

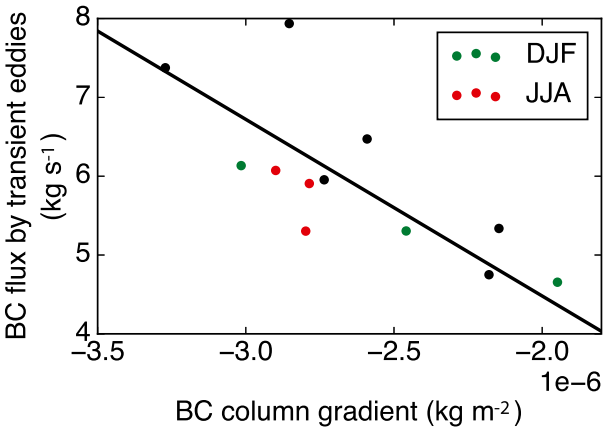

FIG. 5. Scatterplot of vertically integrated monthly mean meridional BC flux by transient eddies vs meridional gradients of BC column burden averaged over 40°–66°N. The linear regression line is also shown. Green and red dots represent DJF and JJA, respectively.

JJA when BC from all regions experiences diabatic heating and wet removal caused by precipitation, the flux has only one notable peak at about 800 hPa originating from anthropogenic emissions in Europe and boreal forest fires over Eurasia. BC from North America and East Asia is more likely to be transported diabatically to higher altitudes, and diluted and rained out along the path to the Arctic (Klonecki et al. 2003).

We further explore the meridional BC flux in frequency space by applying a time filter. Since the mean meridional flux is negligible, $\{\overline{v_n c_n}\}$ approximates BC transport carried out by eddies with time scales greater than $2n$ days (Hall et al. 1994). Note that the subscript n denotes means of consecutive nonoverlapping n-day periods. Figure 4 shows the time-filtered BC flux into the Arctic as a fraction of the total flux. The relative contributions from eddies of different frequencies to the total BC transport are different in the two seasons. In DJF, about 90% of the BC flux is realized by eddies with time scales longer than 10 days. Slightly more than 40% of the BC flux arises from eddies that persist longer than 60 days. In contrast, eddies with time scales longer than 10 days account for less than 50% of the JJA flux, and eddies that persist longer than 60 days have very little contribution to the total flux. Thus, while synoptic eddies dominate in JJA, low-frequency eddies contribute substantially to the total transport in DJF.

The prominence of transient eddies in all seasons suggests that the long-range transport of Arctic haze can be represented, to first order, as turbulent diffusion of midlatitude sources, despite the complexities at the process level (Shaw 1981). The idea of simplifying eddy transport as turbulent diffusion is widely used in understanding the atmospheric transport of heat and potential vorticity (Held 1999). Here we apply it to study tracer transport. For a local downgradient diffusion process, the vertically integrated meridional transient eddy BC flux can be assumed to be proportional to the meridional gradient of the BC column burden:

$$\{\overline{v'c'}\} = -D\frac{\partial}{\partial y}\{\overline{c}\}, \tag{7}$$

where D is the turbulent diffusivity. It is clear from Fig. 5 that there is a strong negative correlation ($r = -0.75$) between the transient eddy flux and meridional gradient averaged at a number of latitudes between 40° and 66°N, which validates the diffusive picture of pollution transport. The magnitude of the slope of the best linear fit with zero intercept ($2.24 \times 10^6\,\mathrm{m^2\,s^{-1}}$) represents the eddy diffusivity, which is within the range of the estimated values in previous studies (e.g., Bolin and Keeling 1963; Newell et al. 1969; Held 1999). While BC sources and sinks vary throughout the year, the eddy diffusivity does not change substantially with the season. This indicates that the diffusivity is intrinsically determined by atmospheric dynamics rather than specific tracer properties. It would be interesting to see whether this result is robust across different models.

It should be noted that besides the large-scale circulation patterns, BC emissions also play a role in determining the BC flux into the Arctic. Most of the Arctic BC comes from anthropogenic emissions from midlatitude industrial regions and biomass burning

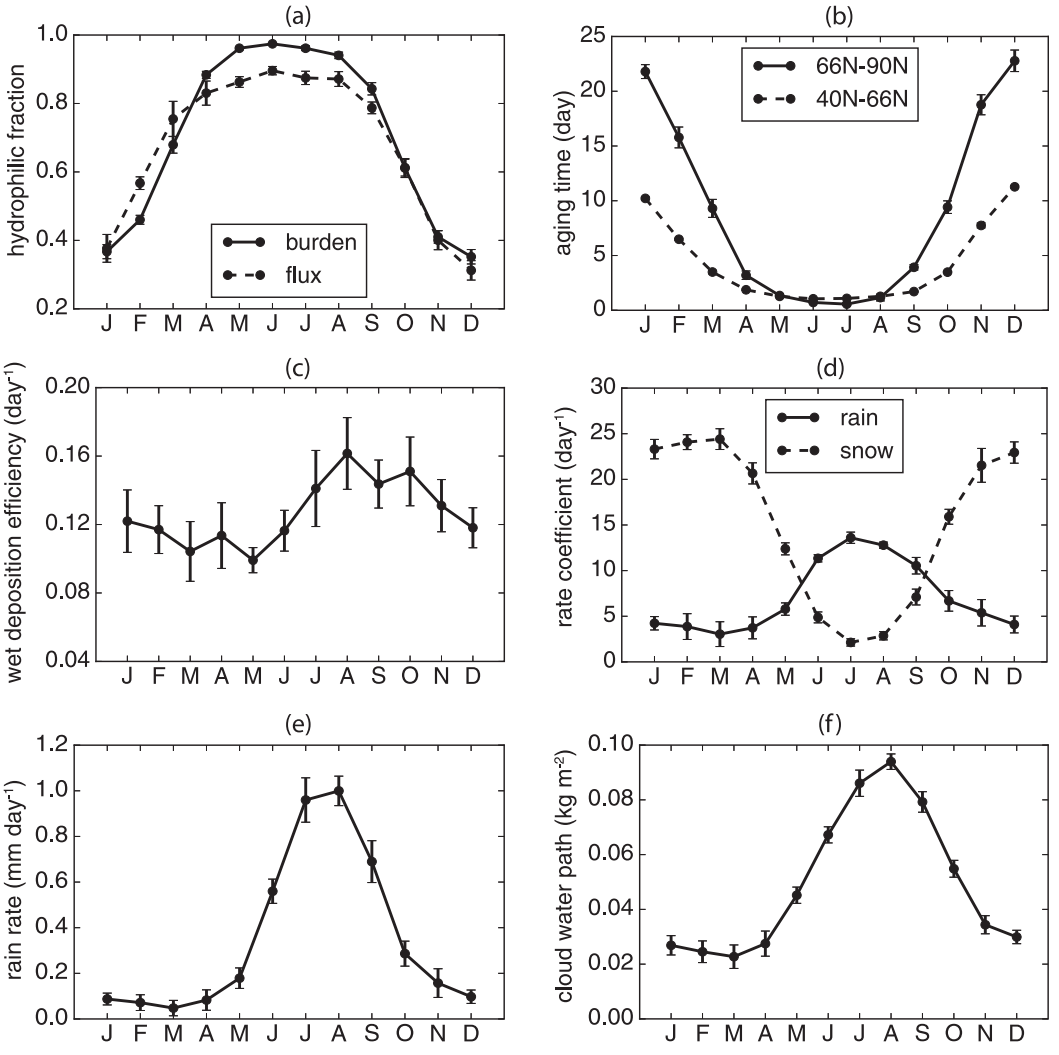

FIG. 6. Monthly mean AM3-simulated (a) hydrophilic fractions of Arctic BC (solid) and BC flux into the Arctic (dashed), (b) BC aging time averaged at 66°–90°N (solid) and 40°–66°N (dashed), (c) Arctic BCpi wet deposition efficiency, (d) rate coefficients of conversion of cloud condensate to rain (solid) and snow (dashed) in the Arctic, (e) Arctic rain rate, and (f) Arctic cloud water path. Error bars denote one std dev from monthly means.

emissions from boreal forest, which have opposite seasonal variations. Anthropogenic emissions are highest during the heating season from November to March, whereas biomass burning emissions are highest from April to August. The total BC emission in the mid-to-high latitudes used in this study has a weak seasonal cycle with a maximum in April and a minimum in September (not shown). This explains some of the difference in the total BC flux between spring and autumn (Fig. 2b).

6. Hydrophilic fraction

Figure 6a (solid line) shows the monthly mean hydrophilic fraction r of Arctic BC, which has a pronounced seasonal cycle. The hydrophilic fraction in DJF is only approximately 40%, while almost all BC is hydrophilic in JJA. Figure 6a (dashed line) shows the monthly mean hydrophilic fraction of the meridional BC flux into the Arctic (i.e., the ratio of BCpi flux to total BC flux), which is very similar to that of Arctic BC. This indicates that the transformation from hydrophobic to hydrophilic BC occurs mainly during the long-range transport, and the seasonal cycle of the Arctic BC hydrophilic fraction is shaped mainly by the aging process along the long-range transport path rather than locally in the Arctic.

Figure 6b shows the monthly mean e-folding aging time of BC (the inverse of the aging rate coefficient, computed as the average BCpo concentration divided

by the average conversion rate from BCpo to BCpi) at 40°–66°N and over the Arctic. During the transport from midlatitudes to the Arctic, the average aging time is much longer in DJF (~10 days) than in JJA (~1 day), resulting in a substantially lower hydrophilic fraction in winter. In the Arctic, the seasonal variations of BC aging time are even greater, which further amplifies the seasonal cycle of the hydrophilic fraction, as shown by the difference between the solid and dashed lines in Fig. 6a.

The parameterized aging scheme in the model (section 2) accounts for the seasonal cycle of the aging process and thus the hydrophilic fraction. The aging rate due to condensation is proportional to OH concentrations. As a result of enhanced solar radiation and specific humidity, OH concentrations are much higher in JJA than in DJF, resulting in more rapid aging by condensation in summer. The aging occurring through other processes (e.g., coagulation) is assumed to have a fixed *e*-folding time of 20 days, which is longer than that for the aging via condensation during the long-range transport (Fig. 6b, dashed line), and thus does not contribute to the seasonal cycle of the hydrophilic fraction.

The change in the hydrophilic fraction also helps explain the change in Arctic BC during spring and fall. From October to November, there is a sharp decrease in the hydrophilic fraction, resulting in a rapid buildup of BC. Similarly, from March to April, the increase in the hydrophilic fraction contributes to the decline in BC concentrations. The hydrophilic fraction, however, is fairly constant from April to September, in contrast with the continuous decrease in BC starting from April. The wet deposition efficiency plays an important role in driving BC changes during this time period, as discussed in the next section.

7. BCpi wet deposition efficiency

Figure 6c shows the monthly mean wet deposition efficiency of BCpi (w) in the Arctic. The wet deposition efficiency in JJA is about 20% higher than in DJF, contributing to the lower BC in JJA than in DJF. The magnitude of its seasonal cycle, however, is much weaker than that of the hydrophilic fraction r (Fig. 6a). Yet, the wet deposition efficiency increases continuously by a factor of 2 from May to August, driving the transition from moderate BC burdens in late spring to exceedingly low burdens in summer.

The wet deposition efficiency is largely controlled by the in-cloud scavenging rate coefficient k_{scav} [in Eq. (2)]. To better understand the factors determining k_{scav}, we analyze the conversion rate coefficients of cloud condensate to rain k_{rain} and snow k_{snow} through which in-cloud scavenging occurs, which are defined as

$$k_{rain} = \frac{P_{rain}}{Q_{liq} + Q_{ice}} \quad \text{and} \quad k_{snow} = \frac{P_{snow}}{Q_{liq} + Q_{ice}}. \quad (8)$$

In this study we use a much larger scavenging efficiency for rain than for snow produced by Bergeron process. Therefore according to Eq. (2), k_{scav} and thus the wet deposition efficiency are determined by k_{rain} rather than k_{snow} when most snow is produced by the Bergeron process, which is the case for the Arctic during the winter (Fan et al. 2012). Figure 6d shows the annual cycle of AM3-simulated k_{rain} and k_{snow} in the Arctic. [Note that P_{rain}, P_{snow}, Q_{liq}, and Q_{ice} are first averaged over the Arctic and then k_{rain} and k_{snow} are calculated using Eq. (8).] Consistent with the seasonal cycle of the wet deposition efficiency, k_{rain} is higher in JJA than in DJF. From May to August, k_{rain} increases by a factor of 2, which helps explain the twofold increase in the wet deposition efficiency. The seasonal variation in k_{rain} is a result of the seasonal cycle of both rain rate P_{rain} and cloud water content $Q_{liq} + Q_{ice}$. As the atmosphere becomes warmer and holds more water vapor from DJF to JJA, P_{rain} increases by about an order of magnitude (Fig. 6e) due to thermodynamic reasons. However, k_{rain} and the wet deposition efficiency increase by only less than a factor of 2. This is because $Q_{liq} + Q_{ice}$ increases by a factor of 4–5 (Fig. 6f) from DJF to JJA as the clouds become more vigorous, and the wet deposition efficiency is determined by the ratio of P_{rain} to $Q_{liq} + Q_{ice}$ rather than by P_{rain} alone.

In contrast with k_{rain}, k_{snow} is much larger in DJF than in JJA because cold temperature favors snow formation, which is opposite to the seasonal variations in the wet deposition efficiency. Therefore one may expect that models without different removal efficiencies for liquid and mixed-phase clouds cannot reproduce the seasonal cycle of the wet deposition efficiency, and thus the seasonal cycle of Arctic BC concentrations.

It should be noted that as clouds get warmer and contain more liquid water from DJF to JJA, riming overtakes the Bergeron process as the main mechanism for generating snow in the Arctic. In AM3 riming accounts for about 20% and 80% of the total Arctic snow production in DJF and JJA, respectively (not shown). In this study riming is assumed to be as efficient at removing aerosols as rain. The change in the mechanism of snow production, however, does not have a strong effect on the seasonal cycle of the wet deposition efficiency. Since k_{snow} is larger in DJF than in JJA by almost an order of magnitude (Fig. 6d), the conversion rate coefficient of cloud condensate to snow produced by

riming (i.e., k_{snow} scaled by the riming fraction) reaches a maximum in winter, despite much higher riming fraction in summer. The conversion of cloud condensate to rain is much faster than to snow in summer, indicating that rain is the dominant removal mechanism. As a result, we conclude that the difference in the scavenging efficiency between rain and snow is the primary cause of the seasonal cycle of the wet deposition efficiency, and the change in the dominant mechanism of snow production is a secondary consideration.

8. Concluding remarks

It has long been recognized that aerosols from midlatitude source regions undergo long-range transport, leading to high concentrations of air pollution in the Arctic during late winter and early spring. Here we apply the GFDL AM3 to analyze the key factors affecting the seasonal variations in Arctic BC. The model is able to reproduce the observed Arctic BC concentrations and seasonality, with 3–4 times higher values in DJF than in JJA. We find that the seasonal cycle of Arctic BC is caused mainly by the seasonality of wet deposition, with a secondary contribution from the long-range transport flux.

The transport of BC at mid-to-high latitudes occurs mainly through stationary and transient eddies, rather than through the mean meridional circulation. Stationary eddies account for approximately 40% of the total flux in DJF, while virtually all the transport is realized through transient eddies in JJA. The vertical distribution of meridional BC transport also varies seasonally. The vertical profile of the BC flux into the Arctic in DJF has two peaks (one in the boundary layer and the other in the midtroposphere), whereas the BC flux in JJA is concentrated in the lower troposphere. The total meridional BC flux into the Arctic, however, changes little throughout the year despite the shift in large-scale circulation.

The wet removal depends on both BC hydrophilic fraction and BCpi wet deposition efficiency. The hydrophilic fraction is smaller in DJF than in JJA because of the slower BC aging along the long-range transport path to the Arctic during winter. This difference in the hydrophilic fraction plays a dominant role in the large difference in BC concentrations between DJF and JJA. The wet deposition efficiency is lower in DJF mainly because snow produced in mixed-phase clouds is less efficient in removing BC than rain. The decrease in BC concentrations from late spring to summer is due to a gradual but steady increase in the wet deposition efficiency, while the return of BC in late autumn is caused mainly by a sharp decrease in the hydrophilic fraction.

Our results are consistent with the observational analysis of Garrett et al. (2011), which argued that some combination of dry deposition and wet scavenging drives the seasonal cycle of aerosols at low altitudes in the North American Arctic. Here we show that the dominance of wet deposition in determining BC seasonal cycle applies to the entire Arctic. We further explain the seasonality of wet deposition in terms of aging and cloud microphysical processes. While being influenced by complicated physical and chemical factors, these processes are parameterized in the model in a relatively simple way. Measurements of Arctic BC mixing state at different times are required for verifying the assumed OH dependence of the aging rate. Measurements of BC wet deposition and concentrations in rain and snow will be particularly useful for constraining the rain and snow scavenging efficiencies. It should also be noted that besides transport and wet deposition, large uncertainties remain in BC emission inventories, which have not been discussed in this paper. High-latitude BC emissions from gas flaring and residential combustion have a large contribution to Arctic BC concentrations and are potentially crucial for affecting its seasonality (Stohl et al. 2013). Although these sources are included in HTAP emissions, the low biases in model-simulated BC surface concentrations at Alert and Barrow suggest an underestimate of BC emissions at high latitudes. However, as most of the emissions remain close to the surface, their contributions to BC in the middle and upper troposphere in the Arctic are small (Stohl et al. 2013), and will not affect our conclusions, which are based on BC column burden.

In this study the quantitative analysis of the controlling factors is for BC column burden, as opposed to surface concentration. While they share a similar seasonal cycle, the relative importance of the controlling factors is somewhat different. As shown in Fig. 3, the BC flux in the boundary layer (below 900 hPa) in winter is 2–3 times larger than that in summer, contributing to higher surface concentrations. Furthermore, a sensitivity test (not shown) suggests that dry deposition is a very important controlling factor of BC surface concentrations, while wet deposition plays less of a role than it does in causing high BC column burdens in winter.

Although the analysis in this paper focuses on BC, the findings should be generally applicable to other components of Arctic haze. For example, sulfate has a similar seasonal cycle, but with peak concentrations in spring as opposed to winter (as is the case for BC) (Shindell et al. 2008). The difference in the scavenging efficiencies by rain and snow probably dominates the seasonal variations in sulfate. Reducing wet deposition

by snow has been found to improve the model's ability to reproduce the observed sulfate concentrations over the United States (Paulot et al. 2016) and in the Arctic (Browse et al. 2012). The shift in the peak may be due to the absence of an aging process since all sulfate is hydrophilic. The seasonal cycle of sulfate production by SO_2 oxidation may also plays a role in shaping the high sulfate concentrations in spring.

The results discussed here may have implications for understanding the variability and trend in Arctic aerosols and their climate impacts. Since large-scale circulation influences the key processes of long-range transport and the spatial pattern of precipitation, natural climate variability at annual to decadal time scales may play an important role in determining changes in aerosol concentrations in the Arctic (Christoudias et al. 2012; Eckhardt et al. 2003). It would be interesting to apply our analysis to study the effect of climate variability on the characteristics of atmospheric transport and wet deposition. As climate warms, precipitation at high latitudes is expected to increase, but the fraction of snow may decrease (Barnett et al. 2005; Singarayer et al. 2006). These changes tend to enhance the wet scavenging of aerosols and result in a cleaner Arctic atmosphere. A recent study has shown that with constant BC emissions, the annual mean Arctic BC burden will be reduced by 13.6% by the end of the twenty-first century because of the enhanced wet removal in a warmer climate (Jiao and Flanner 2016). The aging process, which is affected by atmospheric composition, may also vary over time. SO_2 emissions at midlatitudes have generally declined in recent decades (Streets et al. 2006) and are projected to decrease even more in the future (Levy et al. 2008). This long-term trend in SO_2 emissions will result in a decrease in sulfate concentrations but an increase in BC concentrations in the Arctic because of a slower aging process by condensation of H_2SO_4 and thus weaker wet removal. Therefore it is important to consider the changes in aerosol sources and sinks when using models to examine how aerosols may alter Arctic climate under future emission scenarios.

Acknowledgments. Songmiao Fan and Fabien Paulot provided helpful reviews of an earlier draft. We thank three anonymous reviewers for their thoughtful comments and helpful suggestions. We acknowledge the Science and Technology Branch at Environment and Climate Change Canada, the Global Monitoring Division at NOAA/Earth System Research Laboratory, and Norwegian Institute for Atmospheric Research for providing measurement data. The observations at Alert, Barrow, and Zeppelin are available through the Canadian Aerosol Baseline Measurement (CABM) Program datasets (http://www.ec.gc.ca/donneesnatchem-natchemdata/default.asp?lang=En&n=22F5B2D4-1), the ESRL/GMD ftp site (/ftp.cmdl.noaa.gov/aerosol/brw/archive/), and World Data Centre for Aerosols (EBAS) (http://ebas.nilu.no). The HIPPO data (Wofsy et al. 2012) are available at the CDIAC HIPPO data archive (http://hippo.ornl.gov/10secdownload/). Model simulations are archived at GFDL and are available from the authors upon request. Zhaoyi Shen is supported by the National Oceanic and Atmospheric Administration, U.S. Department of Commerce under Award NA14OAR4320106. The statements, findings, conclusions, and recommendations are those of the authors and do not necessarily reflect the views of the National Oceanic and Atmospheric Administration, or the U.S. Department of Commerce.

REFERENCES

Barnett, T. P., J. C. Adam, and D. P. Lettenmaier, 2005: Potential impacts of a warming climate on water availability in snow-dominated regions. *Nature*, **438**, 303–309, doi:10.1038/nature04141.

Barrie, L. A., 1986: Arctic air pollution: An overview of current knowledge. *Atmos. Environ.*, **20**, 643–663, doi:10.1016/0004-6981(86)90180-0.

Bindoff, N., and Coauthors, 2013: Detection and attribution of climate change: From global to regional. *Climate Change 2013: The Physical Science Basis*, Cambridge University Press, 867–952, doi:10.1017/CBO9781107415324.022.

Bolin, B., and C. D. Keeling, 1963: Large-scale atmospheric mixing as deduced from the seasonal and meridional variations of carbon dioxide. *J. Geophys. Res.*, **68**, 3899–3920, doi:10.1029/JZ068i013p03899.

Bond, T. C., and Coauthors, 2013: Bounding the role of black carbon in the climate system: A scientific assessment. *J. Geophys. Res. Atmos.*, **118**, 5380–5552, doi:10.1002/jgrd.50171.

Bourgeois, Q., and I. Bey, 2011: Pollution transport efficiency toward the Arctic: Sensitivity to aerosol scavenging and source regions. *J. Geophys. Res.*, **116**, D08213, doi:10.1029/2010JD015096.

Browse, J., K. S. Carslaw, S. R. Arnold, K. Pringle, and O. Boucher, 2012: The scavenging processes controlling the seasonal cycle in Arctic sulphate and black carbon aerosol. *Atmos. Chem. Phys.*, **12**, 6775–6798, doi:10.5194/acp-12-6775-2012.

Christoudias, T., A. Pozzer, and J. Lelieveld, 2012: Influence of the North Atlantic Oscillation on air pollution transport. *Atmos. Chem. Phys.*, **12**, 869–877, doi:10.5194/acp-12-869-2012.

Cozic, J., S. Mertes, B. Verheggen, D. J. Cziczo, S. J. Gallavardin, S. Walter, U. Baltensperger, and E. Weingartner, 2008: Black carbon enrichment in atmospheric ice particle residuals observed in lower tropospheric mixed phase clouds. *J. Geophys. Res.*, **113**, D15209, doi:10.1029/2007JD009266.

Donner, L. J., and Coauthors, 2011: The dynamical core, physical parameterizations, and basic simulation characteristics of the atmospheric component AM3 of the GFDL global coupled model CM3. *J. Climate*, **24**, 3484–3519, doi:10.1175/2011JCLI3955.1.

Eckhardt, S., and Coauthors, 2003: The North Atlantic Oscillation controls air pollution transport to the Arctic. *Atmos. Chem. Phys.*, **3**, 1769–1778, doi:10.5194/acp-3-1769-2003.

——, and Coauthors, 2015: Current model capabilities for simulating black carbon and sulfate concentrations in the Arctic atmosphere: A multi-model evaluation using a comprehensive measurement data set. *Atmos. Chem. Phys.*, **15**, 9413–9433, doi:10.5194/acp-15-9413-2015.

Eleftheriadis, K., S. Vratolis, and S. Nyeki, 2009: Aerosol black carbon in the European Arctic: Measurements at Zeppelin station, Ny-Ålesund, Svalbard from 1998–2007. *Geophys. Res. Lett.*, **36**, L02809, doi:10.1029/2008GL035741.

Fan, S.-M., and Coauthors, 2012: Inferring ice formation processes from global-scale black carbon profiles observed in the remote atmosphere and model simulations. *J. Geophys. Res.*, **117**, D23205, doi:10.1029/2012JD018126.

Friedman, B., G. Kulkarni, J. Beránek, A. Zelenyuk, J. A. Thornton, and D. J. Cziczo, 2011: Ice nucleation and droplet formation by bare and coated soot particles. *J. Geophys. Res.*, **116**, D17203, doi:10.1029/2011JD015999.

Gallagher, M. W., 2002: Measurements and parameterizations of small aerosol deposition velocities to grassland, arable crops, and forest: Influence of surface roughness length on deposition. *J. Geophys. Res.*, **107**, 4154, doi:10.1029/2001JD000817.

Garrett, T. J., and L. L. Verzella, 2008: Looking back: An evolving history of Arctic aerosols. *Bull. Amer. Meteor. Soc.*, **89**, 299–302, doi:10.1175/BAMS-89-3-299.

——, S. Brattström, S. Sharma, D. E. J. Worthy, and P. Novelli, 2011: The role of scavenging in the seasonal transport of black carbon and sulfate to the Arctic. *Geophys. Res. Lett.*, **38**, L16805, doi:10.1029/2011GL048221.

Hall, N. M. J., B. J. Hoskins, P. J. Valdes, and C. A. Senior, 1994: Storm tracks in a high-resolution GCM with doubled carbon dioxide. *Quart. J. Roy. Meteor. Soc.*, **120**, 1209–1230, doi:10.1002/qj.49712051905.

Held, I. M., 1999: The macroturbulence of the troposphere. *Tellus*, **51A**, 59–70, doi:10.3402/tellusa.v51i1.12306.

Huang, L., S. L. Gong, C. Q. Jia, and D. Lavoué, 2010: Importance of deposition processes in simulating the seasonality of the Arctic black carbon aerosol. *J. Geophys. Res.*, **115**, D17207, doi:10.1029/2009JD013478.

Iversen, T., and E. Joranger, 1985: Arctic air pollution and large scale atmospheric flows. *Atmos. Environ.*, **19**, 2099–2108, doi:10.1016/0004-6981(85)90117-9.

Janssens-Maenhout, G., and Coauthors, 2015: HTAP_v2.2: A mosaic of regional and global emission grid maps for 2008 and 2010 to study hemispheric transport of air pollution. *Atmos. Chem. Phys.*, **15**, 11 411–11 432, doi:10.5194/acp-15-11411-2015.

Jiao, C., and M. G. Flanner, 2016: Changing black carbon transport to the Arctic from present day to the end of 21st century. *J. Geophys. Res. Atmos.*, **121**, 4734–4750, doi:10.1002/2015JD023964.

Klonecki, A., P. Hess, L. Emmons, L. Smith, J. Orlando, and D. Blake, 2003: Seasonal changes in the transport of pollutants into the Arctic troposphere-model study. *J. Geophys. Res.*, **108**, 8367, doi:10.1029/2002JD002199.

Koch, D., 2001: Transport and direct radiative forcing of carbonaceous and sulfate aerosols in the GISS GCM. *J. Geophys. Res.*, **106**, 20 311–20 332, doi:10.1029/2001JD900038.

——, and J. Hansen, 2005: Distant origins of Arctic black carbon: A Goddard Institute for Space Studies ModelE experiment. *J. Geophys. Res.*, **110**, D04204, doi:10.1029/2004JD005296.

——, and Coauthors, 2009: Evaluation of black carbon estimations in global aerosol models. *Atmos. Chem. Phys.*, **9**, 9001–9026, doi:10.5194/acp-9-9001-2009.

Law, K. S., and A. Stohl, 2007: Arctic air pollution: Origins and impacts. *Science*, **315**, 1537–1540, doi:10.1126/science.1137695.

Levy, H., M. D. Schwarzkopf, L. Horowitz, V. Ramaswamy, and K. L. Findell, 2008: Strong sensitivity of late 21st century climate to projected changes in short-lived air pollutants. *J. Geophys. Res.*, **113**, D06102, doi:10.1029/2007JD009176.

Li, F., P. Ginoux, and V. Ramaswamy, 2008: Distribution, transport, and deposition of mineral dust in the Southern Ocean and Antarctica: Contribution of major sources. *J. Geophys. Res.*, **113**, D10207, doi:10.1029/2007JD009190.

Lin, M., and Coauthors, 2012: Transport of Asian ozone pollution into surface air over the western United States in spring. *J. Geophys. Res.*, **117**, D00V07, doi:10.1029/2011JD016961.

Liu, J., S. Fan, L. W. Horowitz, and H. Levy, 2011: Evaluation of factors controlling long-range transport of black carbon to the Arctic. *J. Geophys. Res.*, **116**, D04307, doi:10.1029/2010JD015145.

Liu, X., P.-L. Ma, H. Wang, S. Tilmes, B. Singh, R. C. Easter, S. J. Ghan, and P. J. Rasch, 2016: Description and evaluation of a new four-mode version of the Modal Aerosol Module (MAM4) within version 5.3 of the Community Atmosphere Model. *Geosci. Model Dev.*, **9**, 505–522, doi:10.5194/gmd-9-505-2016.

Ma, P.-L., and Coauthors, 2013: The role of circulation features on black carbon transport into the Arctic in the Community Atmosphere Model version 5 (CAM5). *J. Geophys. Res. Atmos.*, **118**, 4657–4669, doi:10.1002/jgrd.50411.

Mitchell, J. M., 1957: Visual range in the polar regions with particular reference to the Alaskan Arctic. *J. Atmos. Terr. Phys.* (Special Suppl.), 195–211.

Newell, R. E., D. G. Vincent, and J. W. Kidson, 1969: Interhemispheric mass exchange from meteorological and trace substance observations. *Tellus*, **21A**, 641–647, doi:10.1111/j.2153-3490.1969.tb00471.x.

Oshima, N., M. Koike, Y. Zhang, and Y. Kondo, 2009: Aging of black carbon in outflow from anthropogenic sources using a mixing state resolved model: 2. Aerosol optical properties and cloud condensation nuclei activities. *J. Geophys. Res.*, **114**, D18202, doi:10.1029/2008JD011681.

Paulot, F., and Coauthors, 2016: Sensitivity of nitrate aerosols to ammonia emissions and to nitrate chemistry: Implications for present and future nitrate optical depth. *Atmos. Chem. Phys.*, **16**, 1459–1477, doi:10.5194/acp-16-1459-2016.

Petters, M. D., A. J. Prenni, S. M. Kreidenweis, P. J. DeMott, A. Matsunaga, Y. B. Lim, and P. J. Ziemann, 2006: Chemical aging and the hydrophobic-to-hydrophilic conversion of carbonaceous aerosol. *Geophys. Res. Lett.*, **33**, L24806, doi:10.1029/2006GL027249.

Quinn, P. K., G. Shaw, E. Andrews, E. G. Dutton, T. Ruoho-Airola, and S. L. Gong, 2007: Arctic haze: Current trends and knowledge gaps. *Tellus.*, **59B**, 99–114, doi:10.1111/j.1600-0889.2006.00236.x.

Schulz, M., and Coauthors, 2006: Radiative forcing by aerosols as derived from the AeroCom present-day and pre-industrial simulations. *Atmos. Chem. Phys.*, **6**, 5225–5246, doi:10.5194/acpd-6-5095-2006.

Schwarz, J. P., and Coauthors, 2013: Global-scale seasonally resolved black carbon vertical profiles over the Pacific. *Geophys. Res. Lett.*, **40**, 5542–5547, doi:10.1002/2013GL057775.

Sharma, S., D. Lavoué, H. Cachier, L. A. Barrie, and S. L. Gong, 2004: Long-term trends of the black carbon concentrations in

the Canadian Arctic. *J. Geophys. Res.*, **109**, D15203, doi:10.1029/2003JD004331.

——, E. Andrews, L. A. Barrie, J. A. Ogren, and D. Lavoué, 2006: Variations and sources of the equivalent black carbon in the high Arctic revealed by long-term observations at Alert and Barrow: 1989–2003. *J. Geophys. Res.*, **111**, D14208, doi:10.1029/2005JD006581.

Shaw, G., 1981: Eddy diffusion transport of Arctic pollution from the mid-latitudes: A preliminary model. *Atmos. Environ.*, **15**, 1483–1490, doi:10.1016/0004-6981(81)90356-5.

Shindell, D., and G. Faluvegi, 2009: Climate response to regional radiative forcing during the twentieth century. *Nat. Geosci.*, **2**, 294–300, doi:10.1038/ngeo473.

——, and Coauthors, 2008: A multi-model assessment of pollution transport to the Arctic. *Atmos. Chem. Phys.*, **8**, 5353–5372, doi:10.5194/acp-8-5353-2008.

Singarayer, J. S., J. L. Bamber, and P. J. Valdes, 2006: Twenty-first-century climate impacts from a declining Arctic sea ice cover. *J. Climate*, **19**, 1109–1125, doi:10.1175/JCLI3649.1.

Stohl, A., 2006: Characteristics of atmospheric transport into the Arctic troposphere. *J. Geophys. Res.*, **111**, D11306, doi:10.1029/2005JD006888.

——, Z. Klimont, S. Eckhardt, K. Kupiainen, V. P. Shevchenko, V. M. Kopeikin, and N. Novigatsky, 2013: Black carbon in the Arctic: The underestimated role of gas flaring and residential combustion emissions. *Atmos. Chem. Phys.*, **13**, 8833–8855, doi:10.5194/acp-13-8833-2013.

Streets, D. G., Y. Wu, and M. Chin, 2006: Two-decadal aerosol trends as a likely explanation of the global dimming/brightening transition. *Geophys. Res. Lett.*, **33**, L15806, doi:10.1029/2006GL026471.

Wang, H., and Coauthors, 2013: Sensitivity of remote aerosol distributions to representation of cloud–aerosol interactions in a global climate model. *Geosci. Model Dev.*, **6**, 765–782, doi:10.5194/gmd-6-765-2013.

Wang, Q., and Coauthors, 2014: Global budget and radiative forcing of black carbon aerosol: Constraints from pole-to-pole (HIPPO) observations across the Pacific. *J. Geophys. Res.*, **119**, 195–206, doi:10.1002/2013JD020824.

Wiedinmyer, C., S. K. Akagi, R. J. Yokelson, L. K. Emmons, J. A. Al-Saadi, J. J. Orlando, and J. Soja, 2011: The Fire INventory from NCAR (FINN): A high resolution global model to estimate the emissions from open burning. *Geosci. Model Dev.*, **4**, 625–641, doi:10.5194/gmd-4-625-2011.

Wofsy, S. C., and Coauthors, 2011: HIAPER Pole-to-Pole Observations (HIPPO): Fine-grained, global-scale measurements of climatically important atmospheric gases and aerosols. *Philos. Trans. Roy. Soc. London*, **369A**, 2073–2086, doi:10.1098/rsta.2010.0313.

——, and Coauthors, 2012: HIPPO Merged 10-second Meteorology, Atmospheric Chemistry, and Aerosol Data (release 20121129). Carbon Dioxide Information Analysis Center, Oak Ridge National Laboratory, doi:10.3334/CDIAC/hippo_010.